

Ce:LaBr₃ crystals with SiPM array readout and temperature control for the FAMU experiment at RAL

**M.Bonesini,^{a,1} R.Benocci,^a R.Bertoni,^a M.Clemenza,^a D.Ghittori,^a R.Mazza,^a E.Vallazza,^a
A.deBari,^b A.Menegolli,^b M.Prata,^b M.Rossella,^b M.Baruzzo,^{c,2} E.Mocchiutti^c**

^a*Sezione INFN Milano Bicocca, Dipartimento di Fisica G. Occhialini and Dipartimento di Scienze dell' Ambiente e della Terra, Università di Milano Bicocca, Milano, Italy*

^b*Sezione INFN Pavia and Dipartimento di Fisica, Pavia, Italy*

^c*Sezione INFN Trieste, Trieste, Italy*

E-mail: maurizio.bonesini@mib.infn.it

ABSTRACT: Compact X-rays detectors made of 1/2" Ce:LaBr₃ crystals of cubic shape with SiPM array readout have been developed for the FAMU experiment at RIKEN-RAL, to instrument regions of difficult access. Due to the high photon yield of Ce:LaBr₃ it was possible to use a simple readout scheme based on CAEN V1730 digitizers, without a dedicated amplification stage. The drift with temperature of SiPM gain was corrected by using CAEN A7885D regulated power supply chips with temperature feedback. Energy resolutions (FWHM) around 3.5% at the ¹³⁷Cs peak and around 9% at the ⁵⁷Co peak were obtained.

KEYWORDS: X-ray detectors; PET

¹Corresponding author.

²also at Dipartimento di Scienze Informatiche, Matematiche e Fisiche, Università di Udine.

Contents

1	Introduction	1
2	X-rays detectors with SiPM arrays readout	2
2.1	Temperature control of SiPM gain	4
3	Results from laboratory tests.	6
4	Analysis of performances in beam	6
5	Conclusions	9

1 Introduction

The FAMU (Fisica degli Atomii Muonici) experiment at RAL [1] is designed to measure the hyperfine splitting (HFS) in the ground state (1S) of the muonic hydrogen. It aims at a high accuracy determination of the proton Zemach radius [2], [3]. This experiment may contribute to solve the so-called “proton radius puzzle”: a large and still unsolved disagreement between the proton charge as measured with electrons or muons [4].

A high intensity pulsed low-energy muon beam, stopping in a hydrogen target, is used to produce muonic hydrogen (in a mixture of singlet $F=0$ and triplet $F=1$ states). A tunable mid-IR (MIR) pulsed high power laser then excites the hyperfine splitting (HFS) transition of the 1S muonic hydrogen (from $F=0$ to $F=1$ states). Making use of the muon transfer from muonic hydrogen to another higher-Z gas in the target (such as O_2), the $(\mu^-p)_{1S}$ HFS transition will be recognized by an increase of the number of X-rays from the (μZ^*) cascade, during a laser frequency scan around the resonance value ν_0 ($\Delta E_{HFS} = h\nu_0$). From the measurement of $\Delta E_{HFS}(\mu^-p)_{1S}$ the Zemach radius r_Z of the proton may be computed with a precision up to 5×10^{-3} , thus casting new light on the proton radius puzzle.

The FAMU experiment is performed in steps, starting from the study of the transfer rate from muonic hydrogen to another higher-Z gas and ending with the full working setup including the pump MIR laser and a multipass optical cavity¹. The preliminary steps have allowed to determine the best mixture to be used inside the cryogenic target and optimize the operating conditions. A schematic layout of the experimental setup for the preliminary steps is shown in figure 1.

The RIKEN-RAL muon facility [5] at Rutherford Appleton Laboratory (UK) provides high intensity pulsed muon beams at four experimental ports. The primary proton beam at 800 MeV/c impinges on a secondary carbon target producing pions and then high intensity low energy pulsed muon beams. The muon beams reflect the primary beam structure: two pulses with a 70 ns FWHM and a 320 ns peak to peak distance are delivered, with a 50 Hz repetition rate. The FAMU experiment

¹to enhance the probability of laser light-muon interactions

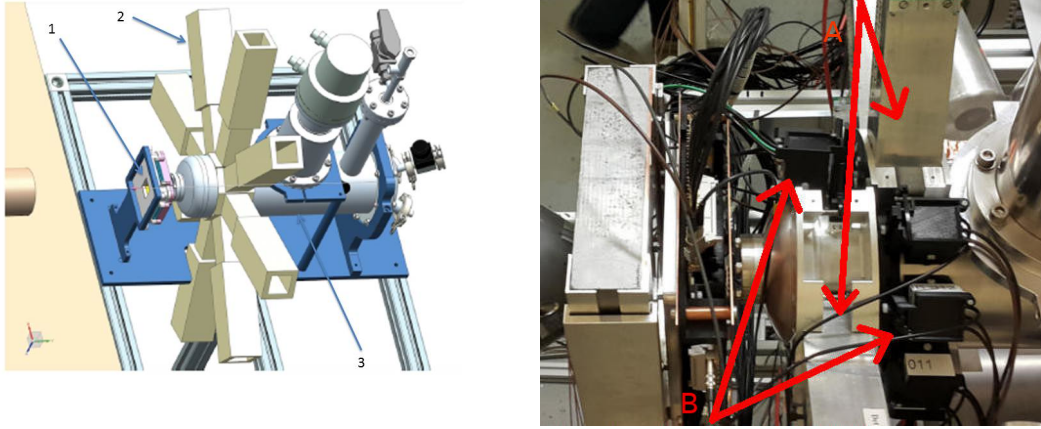


Figure 1. Left panel: layout of the setup for the 2015-2016 data-taking (R582); 1) is the 1 mm pitch beam hodoscope, 2) the crown of eight Ce:LaBr₃ detectors with PMT readout and 3) the cryogenic target. The four HPGe detectors, also used in this run, are not shown. Right panel: picture of the 2018 setup where the two half-crown of the Ce:LaBr₃ detectors with PMT readout (A) were displaced along the beam axis (z) and complemented with 4+4 1/2" Ce:LaBr₃ detectors with SiPM array readout (B).

makes use of a negative decay muon beam at ~ 60 MeV/c. For this experiment, an important issue is the optimal steering of the incoming high intensity pulsed muon beam onto the hydrogen target, to maximize the muonic hydrogen production rate. A system of three beam hodoscopes has been developed for this scope. The first two are based on square 3×3 mm² Bicron BCF12 scintillating fibers read by SiPMs, while the last one is based on square 1×1 mm² scintillating fibers of the same type, with white EMA coating, to avoid light cross-talk [6]. The muon beam intensity is around 6×10^4 μ^- /s in a typical size 4×4 cm². The energy spread is around 10 % and the angular divergence around 60 mrad.

To extract the characteristic muonic X-rays lines (around 100 keV) with a good energy resolution and a minimal events pile-up, a system based on Ce:LaBr₃ crystals and HPGe detectors has been developed. Even if they have better energy resolution, the HPGe detectors are slower, work at cryogenic temperatures and are more expensive. Therefore the main X-rays detector system for the experiment was based on 1" circular Ce:LaBr₃ crystals, 1" long, read by UBA Hamamatsu R11265U-200 PMTs with active divider (up to eight arranged in two detachable half crowns). In addition, an R & D was pursued to complement these detectors with crystals equipped with SiPM readout to instrument regions of more difficult access, see reference [7] for further details.

2 X-rays detectors with SiPM arrays readout

For our aims it is essential to detect low-energy X-rays in the range 100-200 keV. Pr:LuAG [8] and Ce:GAAG [9] crystals with respect to more conventional Ce:LaBr₃, CeBr₃[10] and NaI(Tl) crystals, have the advantage to be non hygroscopic and thus do not need encapsulation.

Results on their performances are reported in references [11], [12]. From laboratory tests a solution based on Ce:LaBr₃ crystals was shown as still to be preferred. A crystal thickness of 0.33 (1.54) cm for 88% attenuation at 100 (200) keV was computed from X-ray attenuation coefficients,

as reported in [13]. It is apparent that for the detection of the O_2 characteristic lines in the region 100-160 keV, corresponding to muon transfer, 1/2" long crystals are adequate. A more complete Monte Carlo simulation based on MNCP[14] provided an estimate of absorption for cubic crystals of 1/2" side with a source at a distance corresponding to the center of the foreseen target. Even in this case 1/2" long crystals were considered adequate.

The structure of a detector with a SiPM array readout is shown in figure 2. The optical contact between the crystal and the SiPM arrays is done through a Bicorn BC631 silicone optical grease. The crystal/PCB holder, realized with a 3D printer, is made in two pieces: one contains the crystal

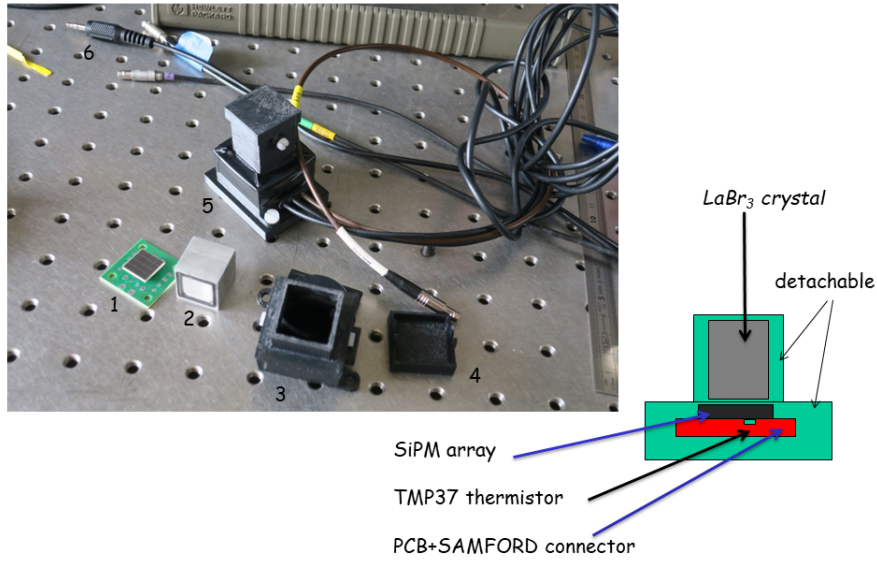


Figure 2. Components of the detectors with SiPM readout. 1) is the Hamamatsu SiPM mounted on the custom PCB, 2) the Ce:LaBr₃ crystal in the Al encapsulation, the optical window is seen in the front. 3) is the holder containing the crystals and the PCB, in two pieces seen from the top. 4) is the cap to guarantee detector's light tightness. The full mounted detector (5) is shown in the back of the picture. The 3.5 mm stereo jack cable (6) connects the temperature sensor (TMP37) on the backside of the SiPM array PCB to the power supply module.

under test, while the other holds the readout electronics with the custom PCB, where a SiPM array is mounted on. The analog signals of the 16 SiPM of one array are summed together on the custom PCB. Signal acquisition may be realized with a standard spectroscopic chain (based on a Ortec 672 spectroscopic amplifier or a fast Ortec 579 Ortec amplifier) or with a fast digitizer. Due to the signal amplitude ($\sim 100 - 200$ mV at the ^{137}Cs peak) no amplification is needed and a direct readout via a digitizer may be used. In our case we made use of a CAEN DT5730 digitizer (desktop version) or a V1730 digitizer (VME format). Both have been used via an optical link and have a bandwidth of 500 MHz with a ± 1 Vpp dynamic range.

In the first instance, we used different 4×4 arrays made from 3×3 mm² SiPM array from Sensl, Advansid and Hamamatsu for their readout. Their main operation characteristics are resumed in

table 1. Hamamatsu SiPM make use of the TSV (“through Silicon via”) technology that eliminates the need of a wire bonding pad, thus reducing dead space problems. The anode of each channel is traced to the backside pad by TSV. Typical gains are in the range 1.7 to 3×10^6 and depend on the applied overvoltages (ΔV_{ov}), while the dark count rate is around 0.5 Mcps for all the considered SiPM arrays.

Table 1. Main characteristics of the SiPM arrays used for our tests. Photon detection efficiency (PDE) are at typical overvoltage values, at λ_{max} . $V_{op} = V_{bd} + \Delta V_{ov}$ is the typical voltage used in our tests. ΔV_{op} is the variation in the suggested voltages for operations, between the 16 different SiPM making a SiPM array. (E) or (S) are used for an epoxy or silicon window.

	V_{bd} (V)	ΔV_{ov} (V)	V_{op} (V)	$\Delta V_{bd}/\Delta T$ (mV/C)	ΔV_{op} (V)	λ_{max} (nm)	PDE ($\sim \lambda_{max}$)	range (nm)
SenSL Array SB-4-3035-CER	24-25	1-5	26	21.5		420	$\sim 30\%$	300-800
Advansid NUV3S-4x4TD	26	2-6	29	26	≤ 0.4	420	$\sim 43\%$	350-900
Hamamatsu S13361-3050-AE (E)	53 ± 5	~ 3	53.8	54	± 0.05	450	$\sim 35\%$	320-900
Hamamatsu S13361-3050-AS (S)	53 ± 5	~ 3	54.2	54	± 0.05	450	$\sim 35\%$	280-900
Hamamatsu S14161-3050-HS (S)	38	~ 2.7	40.8	34	± 0.05	450	$\sim 50\%$	270-900

Preliminary results obtained with a standard spectroscopic chain were reported in references [11], [12] and show resolution at 662 keV from 3.1% (Ce:LaBr₃ crystals with Hamamatsu S13361-3050-AS SiPM arrays) to 8.4% (NaI crystals with the same readout). At lower X-rays energy (~ 122 keV), FWHM energy resolutions between the different crystals become more compatible: as an example while at 662 keV a Ce:LaBr₃ crystal has a resolution a factor ~ 2 better than a NaI(Tl) crystal, at 122 keV this factor reduces only to $\sim 30\%$.

The best results were obtained with Ce:LaBr₃ crystals with a readout based on Hamamatsu SiPM arrays with a silicone window, that has a better transmission around 380 nm.

As the SiPM gain has a drift with temperature (~ 54 mV/°C for the breakdown voltage of Hamamatsu S13361 SiPM) a temperature correction had to be implemented.

2.1 Temperature control of SiPM gain

The gain of SiPM depends on the applied voltages $V_{op} = V_{bd} + \Delta V_{ov}$ where the overvoltage is kept fixed: typically around $2-4$ V. The breakdown voltage depends from temperature, according to equation:

$$V_{bd}(T) = V_{bd}(T_0) + c \times (T - T_0) \quad (2.1)$$

where c is the temperature coefficient $\Delta V_{bd}/\Delta T$ of table 1 and T_0 a reference temperature, typically 25°C [15]. By correcting for the increase of breakdown voltage with the previous equation 2.1 one may obtain an excellent gain stabilization. The temperature correction may be obtained offline, by recording the temperature, or online with an active feedback.

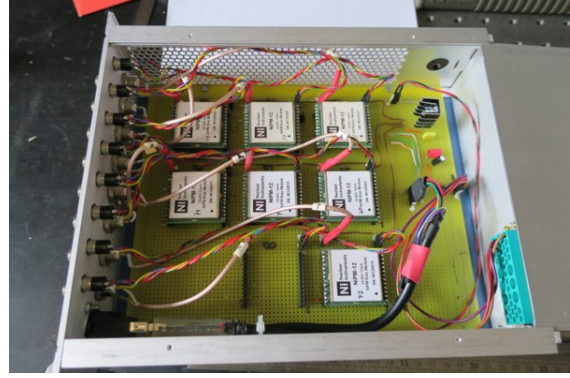
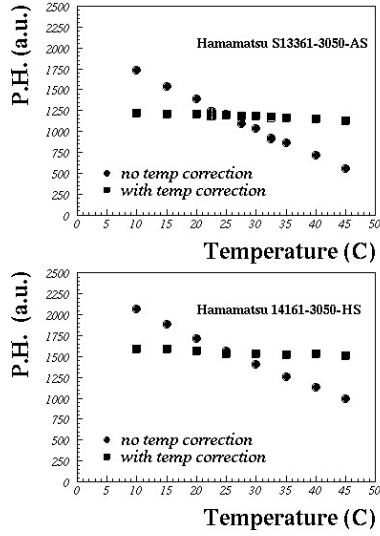


Figure 3. Left panel: P.H. response in a.u. for a typical Ce:LaBr₃ 1/2" crystal as a function of temperature with a ¹³⁷Cs source. Data have been taken inside an IPV30 Memmert climatic chamber, with a temperature resolution $\sim 0.1^\circ\text{C}$. Data have been taken with no temperature correction (circle) and with temperature correction (squares). Right panel: top view of the custom NIM module for temperature control of SiPM gain. The USB-I2C interface is shown in the bottom part of the picture. Seven out of eight CAEN A7585D power supply chips are shown in place. A wire-wrap mounting has been used.

The effect to be corrected is shown in figure 3 (black circles) for two different Hamamatsu SiPM arrays. Data have been taken inside a Memmert IPV30 climatic chamber, with a temperature resolution of 0.1°C between 10°C and 40°C . A typical detector is irradiated with a ¹³⁷Cs source and data are read by a CAEN V1730 digitizer. The position of the pulse height peak is computed and then plotted as a function of temperature. We initially used single desktop power supply CAEN DT5485P², where the temperature feedback was based on a temperature sensor (TMP37 from Analog Devices) put on the backside of the PCB holding the SiPM array (see figure 2 for details). This temperature sensor is connected via a 3.5 mm stereo cable to the power supply module. Between 10°C and 40°C the detector pulse height response had a variation up to 60 %. This effect is reduced to $\sim 6\%$ after temperature correction, via a CAEN DT5485P desktop module.

All results, based on laboratory tests, were made using such modules for powering the SiPM arrays. For the next future we have developed custom made NIM modules with up to eight HV channels each, based on CAEN A7585D chips. The communication with the host computer is done via an I2C protocol, followed by an USB-I2C converter, using on the computer side a proprietary software³ that may control the setting of the power supply chips, monitor their erogated voltages and currents and record results on an Excel file. These modules realized with a wire wrap technique are shown in figure 3 and their use is foreseen for the next spectroscopic run of FAMU in late 2020. In these modules the primary voltage to feed the power supply chips is taken from the NIM backplane and the interface USB-I2C is realized via a FDTI C232HM-EDSHL-0 module. For data

² 0.1 mV (pp) voltage ripple, ± 20 mV setting precision, 1.2 mV setting resolution, with USB control

³ Zeus software from Nuclear Instruments srl.

taken in December 2018 six DT5485P CAEN modules connected to an USB hub were used instead.

3 Results from laboratory tests.

Results for a typical crystal are shown in figure 4 for both linearity and FWHM resolution (in %) using different laboratory sources in the range between 80 and 1300 keV. At the ^{137}Cs peak a resolution $\sim 3.5\%$ was found, compatible with best results with the standard PMT readout. Results

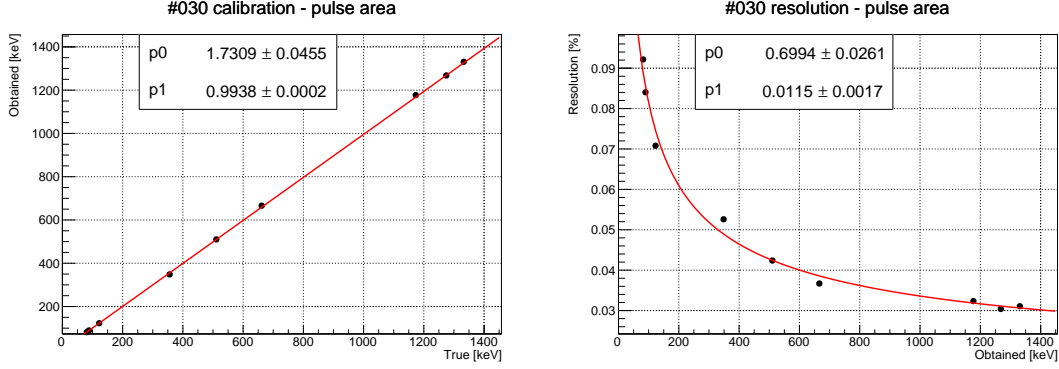


Figure 4. Left panel: linearity for a typical 1/2" Ce:LaBr₃ detectors with SiPM array readout, from OST Photonics (CN). Right panel: FWHM resolution with different test sources for the same detector. Fits are performed with a straight line for linearity and with the expression $p_0 + p_1/\sqrt{E}$ for the FWHM energy resolution.

on linearity and FWHM resolution (%) are also shown in figure 5 for several Ce:LaBr₃ detectors with size $14 \times 14 \times 14 \text{ mm}^3$ from Kinheng Ltd (no. 12-17) and $12 \times 12 \times 12 \text{ mm}^3$ from Ost Photonics (no. 21-32). Detectors with worse energy resolutions are equipped with Hamamatsu S13361 arrays with epoxy windows, that have a reduced transparency to the UV signal emitted from Ce:LaBr₃ or have suffered from ageing problems (such as some older detectors from Kinheng, PRC). Around 122 keV FWHM energy resolutions up to 8% are obtained.

4 Analysis of performances in beam

In the December 2018 run at Port 1 of RIKEN RAL, the two half-crown of 1" Ce:LaBr₃ crystals with PMT readout were displaced of $\sim 10 \text{ cm}$ along the beam direction. They were complemented with four 1/2" Ce:LaBr₃ detectors with SiPM readout, each. The first six detectors were powered via CAEN DT5475 modules with temperature feedback, the last two were powered by conventional ISEG NIM NHS-6001x power supply ⁴ for cross-check. As the temperature in the experimental hall was quite stable (the run was done in winter) no appreciable temperature excursions were seen.

Calibration results in situ with ^{137}Cs , ^{133}Ba , ^{57}Co sources are reported in figure 6 and are roughly compatible with laboratory measurements, even if FWHM resolutions are a little worse. This may be due to worse positioning of sources with respect to the detectors to be calibrated and environmental noise.

⁴ with a voltage ripple less than 2-3 mV, 0.2 mV resolution voltage setting

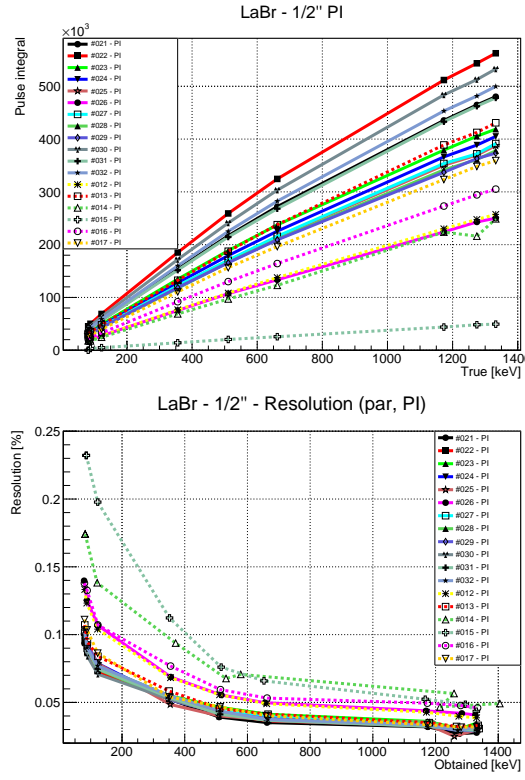


Figure 5. Top panel: linearity for the used 1/2" Ce:LaBr₃ detectors with SiPM array readout. Detectors no. 12-17 are from Kinheng Photonics (PRC), while detectors no. 21-32 are from OST Photonics (PRC). Bottom panel: FWHM resolutions with different test sources for the same detectors.

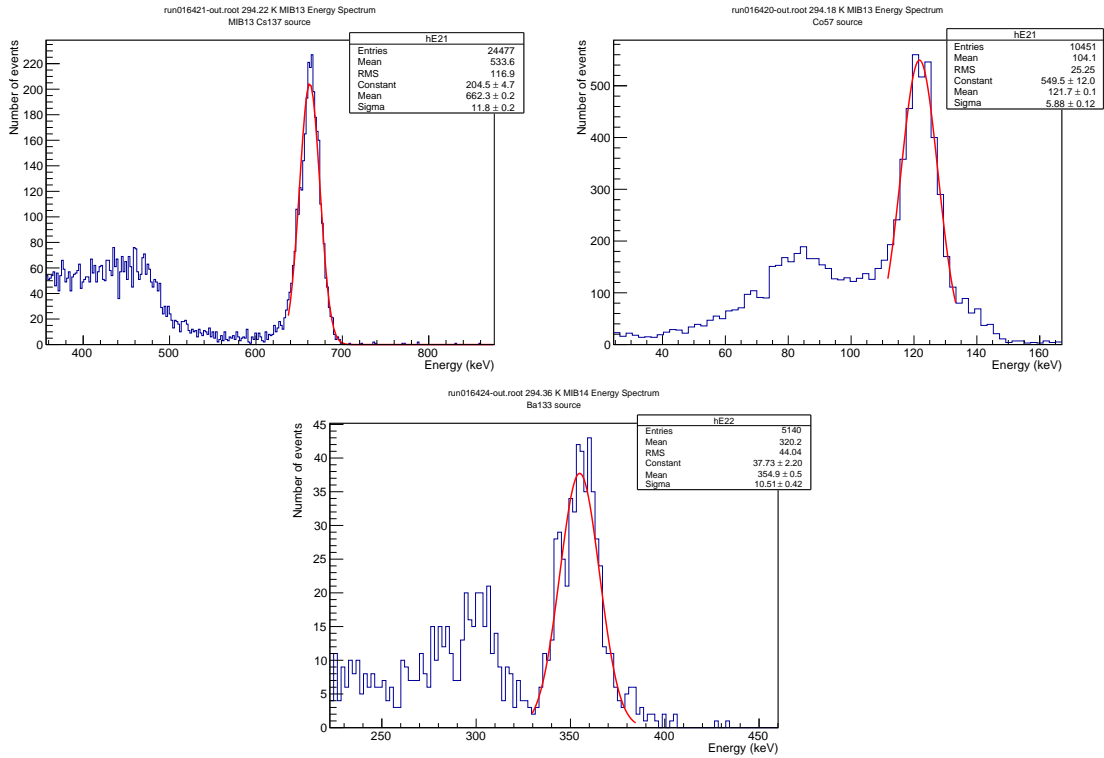


Figure 6. Calibration results obtained with a ¹³⁷Cs, ¹³³Ba and a ⁵⁷Co source during the December 2018 run at RAL. FWHM resolutions are slightly worse as respect to what obtained in laboratory measurements.

Data were then taken with a target filled with pure H_2 for background studies and a mixture of O_2 and H_2 at various concentrations (from 0.3 to 4.6 % weight) at a temperature around 80 K, at various pressures.

The timing properties of one typical detector are shown in figure 7. The two peaks structure of the beam is clearly visible with FWHM and peak-to-peak distance compatible with what expected. In figure 7 the full energy spectrum is reported for the same detector. Characteristic X-rays lines,

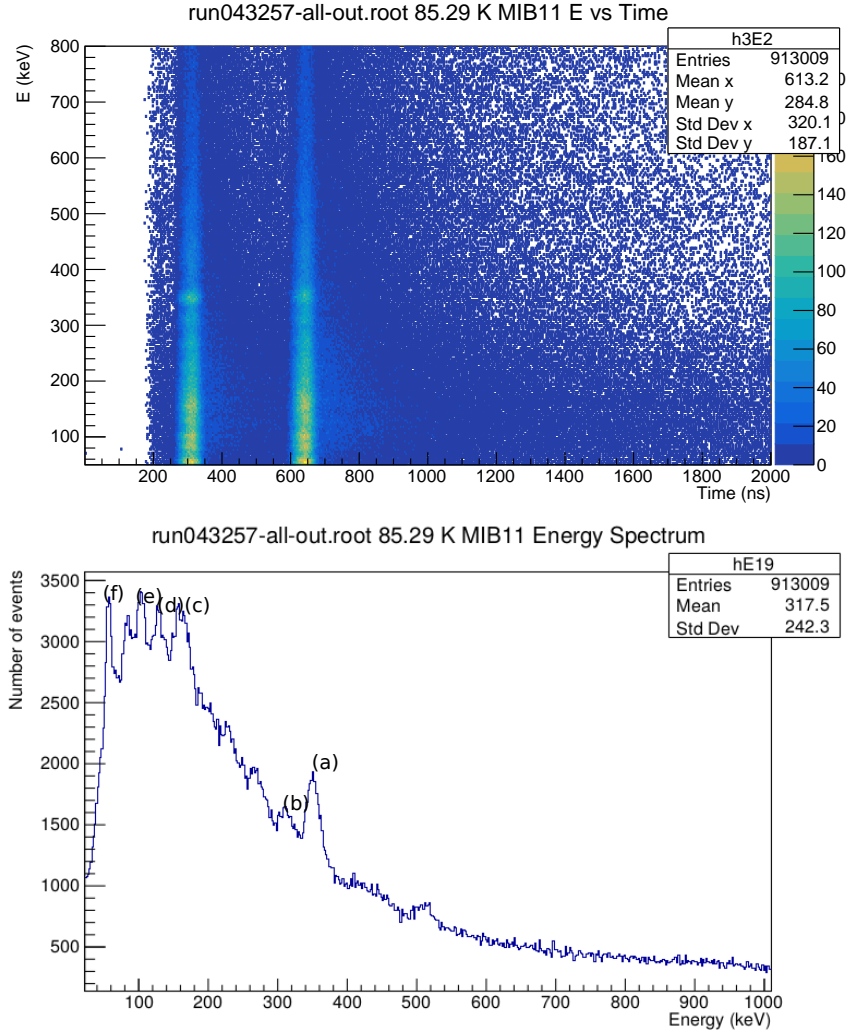


Figure 7. Top panel: X-ray time evolution spectrum of the H_2 -2% O_2 mixture with a 56 MeV/c moun momentum. Bottom panel: energy spectrum for a SiPM array readout 1/2" Ce:LaBr₃ detector using a 2 % O_2 mixture, at 7 bar and 80 K. Background is not subtracted. Characteristic spectral lines at 347 keV and 66 keV from Al (a,f), Nickel at 310 keV and 107 keV (b,e) and Oxygen at 158/167 keV and 133 keV (c,d) may be seen.

mainly Nickel and Aluminium from materials present in the target, are evident from ~ 100 keV to around 400 keV.

5 Conclusions

Ce:LaBr₃ detectors with SiPM array readout and temperature control for the power supply have been assembled and tested both in laboratory, at Sezione INFN Milano Bicocca and in beam at Port 1 at RIKEN RAL. Results show good performances and FWHM resolutions compatible with more bulky conventional detectors with PMT readout. Their use is foreseen, together with the NIM power supply module with temperature feedback, for the coming 2020 FAMU spectroscopic run.

Acknowledgements

We would like to thank S. Banfi, M. Gheigher (INFN Milano Bicocca) for help in mechanics setup. We acknowledge the help of Dr. M. Saviozzi of CAEN, Dr. A. Abba and Dr. V. Arosio of Nuclear Instruments for issues related to the regulated power supply chips for SiPM and their control program Zeus.

References

- [1] A. Vacchi *et al.*, *Measuring the size of the proton*, SPIE Newsroom (2012), DOI:10.1117/2.1201207.004274;
A. Adamczack *et al.*, *Steps towards the hyperfine splitting measurement of the muonic hydrogen ground state: pulsed muon beam and detection system characterization*, JINST **11/05** (2016) P05007;
M. Bonesini, *The FAMU experiment at RIKEN RAL for a precise measure of the proton radius*, PoS(EPS-HEP2019) 132;
C. Pizzolotto *et al.*, *The FAMU experiment: muonic hydrogen high precision spectroscopy studies*, submitted to EPJ A.
- [2] A.C. Zemach, *Proton Structure and the Hyperfine Shift in Hydrogen*, Phys. Rev. **104** (1956) 1771.
- [3] D. Bakalov *et al.*, *Experimental method to measure the hyperfine splitting of muonic hydrogen (μ^-p)_{1S}*, Phys. Lett. **A172** (1993) 277.
- [4] R. Pohl *et al.*, *The size of the proton*, Nature **466** (2010) 213;
A. Antognini *et al.* *Proton Structure from the Measurement of 2S-2P Transition Frequencies of Muonic Hydrogen*, Science **339** (2013) 417
- [5] T. Matsuzaki *et al.*, *The RIKEN RAL pulsed muon facility*, Nucl. Instr. Meth. **A465** (2001) 365.
- [6] R. Carbone *et al.*, *The fiber-SiPM beam monitor of the R484 experiment of the RIKEN-RAL muon facility*, JINST **10** (2015) C03007;
M. Bonesini *et al.*, *The construction of the Fiber-SiPM beam monitor system of the R484 and R582 experiments at RIKEN RAL muon facility*, JINST **12** (2017) C03035;
M. Bonesini *et al.*, *The upgraded beam monitor system of the FAMU experiment at RIKEN-RAL*, Nucl. Instr. Meth **A936** (2019) 592.
- [7] A. Adamczack *et al.*, *The FAMU experiment at RIKEN RAL to study the muon transfer rate from hydrogen to other gases*, JINST **13** (2018) P12033.
- [8] W. Drozdowski *et al.*, *Scintillation Properties of Praseodymium Activated Lu₃Al₅O₁₂ Single Crystals*, IEEE Trans. Nucl. Science **55** (2008) 2429
- [9] J.Y. Yeom *et al.*, *First Performance Results of Ce:GAGG Scintillation Crystals With Silicon Photomultipliers*, IEEE Trans Nucl Science **60**, no.2 (2013) 988.

- [10] F.G.A. Quarati *et al.*, *Scintillation and detection characteristics of high-sensitivity CeBr₃ gamma-ray spectrometers*, Nucl. Instr. Meth. **A729** (2012) 596.
- [11] M. Bonesini *et al.*, *Characterization of new crystals for X-rays detector*, PoS EPS-HEP2015 (2015) 244
- [12] M. Bonesini *et al.*, *Systematic study of innovative hygroscopic and non-hygroscopic crystals with SiPM array readout*, PoS EPS-HEP2017 (2017) 777
- [13] <https://www.nist.gov/pm/x-ray-mass-attenuation-coefficients>;
Handbook of Chemistry and Physics, CRC Press, 67th Edition, 1986.
- [14] L. Carter *et al.*, *Monte Carlo Development in Los Angeles*, LA-5903-MS, 1975.
- [15] A.N. Otte *et al.*, *Characterization of three High Efficiency and Blue Sensitive Silicon Photomultipliers*, Nucl. Instr. Meth. **A846** (2017) 106.